

## Natural and actual valence-band discontinuities in the $a\text{-Si}/a\text{-Si}_{1-x}\text{C}_x\text{:H}$ system: A photoemission study

R.-C. Fang\* and L. Ley†

*Max-Planck-Institut für Festkörperforschung, Heisenbergstrasse 1, Postfach 80 06 65,  
D-7000 Stuttgart 80, Federal Republic of Germany*

(Received 3 April 1989)

We have measured core-level and valence-band spectra of  $a\text{-Si}_{1-x}\text{C}_x$  and  $a\text{-Si}_{1-x}\text{C}_x\text{:H}$  ( $0 \leq x \leq 1$ ), alloys of  $2H\text{-SiC}$ , and of the  $a\text{-Si}/a\text{-Si}_{1-x}\text{C}_x$  and  $a\text{-Si}/a\text{-Si}_{1-x}\text{C}_x\text{:H}$  interfaces. From these measurements we determine the valence-band offsets at the interface  $\Delta E_v$ , the overlayer-induced band bending, and the “natural” band discontinuities  $\Delta E_v^0$ . The latter quantity is defined as the difference in the valence-band maximum of  $a\text{-Si}$  and  $a\text{-Si}_{1-x}\text{C}_x\text{:H}$  when both are referred to the chemically unshifted Si  $2p$  core-level component. It is found that  $\Delta E_v^0$  agrees with  $\Delta E_v$  for  $x < 0.5$  both for the hydrogenated and for dehydrogenated (annealed at  $650^\circ$ ) alloy interfaces. In this range  $\Delta E_v$  is rather insensitive to  $x$  and amounts to 0.8 (with H) and 0.3 eV (without H), respectively. Above  $x = 0.5$ ,  $\Delta E_v$  rises in both cases linearly with  $x$  and reaches values of 2.0 (with H) and 1.5 eV (without H), respectively. These values are smaller than expected for the “natural” offsets and the differences can be accounted for by invoking an interface dipole density of  $3.4 \times 10^{14} e \text{ \AA}/\text{cm}^2$  or a charge transfer of about 0.01 electrons per atom pair across the interface from silicon to the more electronegative  $\text{Si}_{1-x}\text{C}_x$  or  $\text{Si}_{1-x}\text{C}_x\text{:H}$ .

### I. INTRODUCTION

The field of band discontinuities at semiconductor interfaces has reached a certain maturity in the sense that a large body of experimental data is available which gives band offsets that agree to within 0.2–0.3 eV with each other for most well-behaved systems.<sup>1</sup> The experimental situation is matched by theoretical calculations on different levels of sophistication. *Ab initio* self-consistent supercell calculations of lattice-matched and strained interfaces using two different schemes<sup>2–4</sup> yield band offsets in good agreement with experiment except for a few pathological cases. These calculations confirm the experimental observation that band offsets are transitive with the exception of systems containing CuBr (Ref. 5) and do not (on the scale of 0.05–0.1 eV) depend on interface orientation.<sup>6</sup> These two factors imply that the band lineup between two semiconductors  $A$  and  $B$  is determined by the bulk electronic structure of  $A$  and  $B$  and not by the details of the atomic arrangement at the interface as long as no electrically active interface states are created.<sup>5</sup> As a consequence, a number of model theories have been developed that relate the band edges of any given material to a bulk reference level such that the proper band offsets are obtained when the reference levels of  $A$  and  $B$  are made to coincide. Such reference levels are, for example, the charge-neutrality level of Flores and Tejedor<sup>7</sup> and Tersoff,<sup>8</sup> and the closely related dielectric midgap energy of Cardona and Christensen,<sup>9</sup> the vacuum level in the model-solid approach of van der Walle and Martin,<sup>3</sup> and an average  $s$ - $p$  hybrid energy as proposed by Harrison.<sup>10,11</sup> Clearly, the advantage is that only one calculation is needed for each material to obtain, in principle, the band lineups of all possible material combinations.

Ideally, one would like to obtain such a common reference level directly from experiment. The early electron-affinity rule was such an attempt<sup>12</sup> which was, however, bound to fail because it did not take the surface dipoles into consideration which determine the electron affinity of any real solid.

Two other purely experimental reference schemes have been proposed. The empirical deep-level model of Langer and Heinrich<sup>13</sup> and Caldas *et al.*<sup>14</sup> that uses the energy of a common impurity level relative to the band edges to line up the energy gaps of two semiconductors appears to work quite well. Finally, we mention the photoemission work of Shih and Spicer,<sup>15</sup> who use the cation core levels in the HgTe-CdTe alloy system to monitor changes in the position of the valence-band maximum (VBM) as a function of composition and determine thus what they call the “natural” valence-band offset between CdTe and HgTe of 0.35 eV. This value agrees with that measured directly for the CdTe/HgTe interface. The term “natural” implies, as in the original model of Harrison,<sup>10</sup> that no interface dipole is formed upon joining the two semiconductors to form the interface. The work to be discussed here represents an extension of the Shih and Spicer approach to the amorphous  $a\text{-Si}_{1-x}\text{C}_x\text{:H}$  system in the sense that we use the chemically unshifted Si  $2p$  core line as a reference level to monitor differences in the valence-band maximum (VBM) with alloy composition and compare these differences with valence-band offsets measured directly on  $a\text{-Si}/[a\text{-Si}_{1-x}\text{C}_x\text{:H}]$  interfaces. We were encouraged to do such a systematic study by the near coincidence in natural valence-band offsets as determined in this way for  $a\text{-Si:H}/a\text{-Si}_3\text{N}_4$  ( $\Delta E_v = 1.2$  eV) (Ref. 16) and  $a\text{-Si:H}/a\text{-SiO}_2$  ( $\Delta E_v = 3.8$  eV) (Ref. 17) with independently measured valence-band discontinuities of

1.4 (Ref. 18), 1.2 (Ref. 19), and of 4.9 eV (Ref. 20), respectively.

These examples also illustrate an important advantage when studying amorphous interfaces, namely, the much larger discontinuities that may be achieved compared to crystalline materials. Heteroepitaxial growth for crystalline semiconductor interfaces requires generally a close match of the crystal structures and the lattice constants of the two materials. This implies that they are also electronically similar with not too different energy gaps and band discontinuities that seldom exceed 1 eV and are more likely to lie between 0 and 0.6 eV.<sup>1</sup> In amorphous heterojunctions these requirements are obviously relaxed and much larger band offsets can be achieved by combining, for example, a semiconductor like Si or Ge with a dielectric like SiO<sub>2</sub> or Si<sub>3</sub>N<sub>4</sub>. This has two advantages. For one, the large offsets are measured with a greater relative accuracy than small ones given a constant absolute accuracy of  $\pm 0.1$  eV obtained typically in photoemission experiments. This is important when comparing measured offsets with theoretical estimates. As a case in point consider the recent revival of the electron-affinity rule by Menéndez.<sup>21</sup> Based on a *statistical* analysis of experimental data versus affinity-rule offsets he comes to the conclusion that the affinity rule holds despite evidence to the contrary in selected experiments specifically designed to test its validity.<sup>22,23</sup> For the same reason (insufficient experimental accuracy in conjunction with small offsets) it was also difficult to assess whether the inclusion of interface dipoles would improve the atomic orbital theory of Harrison.<sup>11</sup>

The second advantage of amorphous systems is closely related to this last point. The model theories that are based on the lineup of charge-neutrality levels to determine the band offsets rely on the high polarizability (assumed to be infinite) of the semiconductors forming the interface in order to screen differences in their average electronegativities.<sup>8,9</sup> The possibility to form amorphous alloys of any composition could be used to change the polarizability of one part of a heterojunction from *a*-Si with a dielectric constant of about 12 to *a*-SiO<sub>2</sub> with  $\epsilon=4.4$ , for example, and thereby reduce the effect of screening-induced interface dipoles. It was indeed the large difference in valence-band offset predicted by Robertson<sup>24</sup> for the Si/SiC interface with ( $\Delta E_v=0.4$  eV) and without an interface dipole ( $\Delta E_v=1.2$  eV) which led us to investigate the *a*-Si/*a*-Si<sub>1-x</sub>C<sub>x</sub> system.

The use of amorphous interfaces for the study of band offsets also has, however, its drawbacks. Most important is probably the lack of any realistic theoretical treatment comparable to the highly sophisticated *ab initio* calculations of Christensen<sup>4</sup> and van der Walle and Martin<sup>2,3</sup> for crystalline heterojunctions. Such calculations are also not likely to appear for some time to come. On the experimental side are the notorious sensitivity of band gaps and thus band energies on preparation conditions and our lack of knowledge about the detailed microscopic structure of amorphous interfaces. It is therefore mandatory in a study like this to compare band-edge and core-level energies of pure alloys and interfaces for systems prepared under identical conditions. This also alleviates

some of the uncertainties that are introduced when, for example, the VBM is determined from a photoemission spectrum that shows considerable tailing as is often observed in amorphous materials.

The work presented here is thus exploratory in the sense that we try to address some of the questions just raised. Earlier work on *a*-Si:H/*a*-Si<sub>1-x</sub>C<sub>x</sub>:H interfaces has been reviewed by Evangelisti.<sup>25</sup> After a discussion of the experimental setup and the sample preparation in Sec. II we discuss the electronic structure of *a*-Si<sub>1-x</sub>C<sub>x</sub> with and without hydrogen for  $0 \leq x \leq 1$  in Sec. III. Emphasis is placed on defining the chemically unshifted Si 2*p* core level as a reference level to monitor changes in the VBM with alloy composition and hydrogen content. This procedure defines the natural valence-band offset as introduced by Shih and Spicer.<sup>15</sup>

In Sec. IV we investigate the formation of a series of *a*-Si/*a*-Si<sub>1-x</sub>C<sub>x</sub>:H interfaces and measure their valence-band discontinuities. They are compared with the natural offsets in Sec. V where we also draw some general conclusions.

## II. EXPERIMENTAL DETAILS AND SAMPLE PREPARATION

The photoemission measurements were performed with Al *K* $\alpha$  x rays ( $h\nu=1486.6$  eV) for the core levels at a resolution of 1.0 eV and with He I ( $h\nu=21.2$  eV) and He II ( $h\nu=40.8$  eV) radiation for the valence-band spectra at a resolution of 0.3 eV. The use of line sources for this kind of work has the advantage that spectra taken with different photon energies can be combined without introducing additional errors due to uncertainties in the photon energies. The precision of energy measurements is further enhanced to  $\pm 30$  meV by using a fixed pass energy and referring the retarding voltage at the beginning and end of each scan under computer control to a voltmeter with an accuracy of  $2 \times 10^{-5}$ . Samples and interfaces were prepared *in situ* and the specimen could be transferred under ultrahigh vacuum into the spectrometer. The amorphous Si<sub>1-x</sub>C<sub>x</sub> alloys were deposited at room temperature (RT) onto Mo substrates by reactive dc sputtering of a *c*-Si target in a mixture of argon and methane (CH<sub>4</sub>). By adjusting the partial pressure of methane, the carbon content could be varied between  $x=0$  and  $x=0.98$ . The *a*-Si overlayers were also deposited by dc sputtering in a second preparation chamber to avoid cross contamination with carbon. A film of Mo sputter deposited onto each specimen at the end of the measurements was used to monitor the position of the Fermi energy  $E_F$  which is the zero of binding energy for all spectra. The films and interfaces so prepared were free of any contamination as confirmed by PES. Peak positions were determined by least-squares fits with a precision of  $\pm 30$  meV.

The carbon content of the alloys was determined from the area ratio of the C 1*s* and Si 2*p* core-level spectra using crystalline SiC as a standard. In *c*-SiC we obtained for the ratio  $I(\text{C } 1s)/I(\text{Si } 2p)=1.45 \pm 0.05$ . The method of sample preparation introduces hydrogen into the samples. Infrared spectra of specimens prepared on Si sub-

strates simultaneously with those used for the photoemission measurements show major absorption bands between 2860 and 2930  $\text{cm}^{-1}$  and at 2030 and 2100  $\text{cm}^{-1}$ . These bands have been identified with C—H (2860–2930  $\text{cm}^{-1}$ ) and Si—H stretching modes in various configurations by a number of authors.<sup>26</sup> The main Si—C stretching mode is observed as a broad band around 750  $\text{cm}^{-1}$ .<sup>27</sup> The integrated absorption strength [ $\int \alpha(\omega)\omega^{-1}d\omega$ ] of the C—H stretching modes amounts to 140  $\text{cm}^{-1}$  and that of the Si—H stretching modes to 360  $\text{cm}^{-1}$  for an alloy with 10% carbon content. We refrain from a further analysis of these values in terms of relative or absolute hydrogen concentrations in view of the uncertainties about the magnitude and constancy of the corresponding oscillator strengths.<sup>27,28</sup> From the photoemission spectra to be discussed later it appears, however, that our films contain less hydrogen than the glow-discharge specimens of Katayama *et al.*<sup>29</sup> Hydrogen starts to evolve from our samples around 500 °C and by heating them up to 650 °C *in vacuo* all hydrogen can be driven out.

### III. RESULTS

#### A. Valence-band spectra of $a\text{-Si}_{1-x}\text{C}_x\text{:H}$

Figure 1 shows the valence-band spectra of selected  $a\text{-Si}_{1-x}\text{C}_x\text{:H}$  films excited with 40.8-eV photons. Also shown for comparison is the spectrum of crystalline SiC in its hexagonal ( $2H$ ) modification. The spectra have been aligned at peak C for better comparison and the energies of characteristic features relative to peak C are given in Table I.

In lieu of electronic structure calculations for the amorphous alloys it is instructive to compare their valence-band spectra with that of the crystalline  $2H$  (wurtzite) SiC sample and the calculated density of states (DOS) for the cubic (zinc-blende)  $\beta\text{-SiC}$  modification due to Robertson.<sup>30</sup> Both structures consist of a tetrahedral arrangement of Si and C atoms and differ only in the relative orientation of neighboring tetrahedra along a connecting bond: staggered for the cubic or zinc blende and eclipsed for the hexagonal or wurtzite structure.

We identify three major structures A, B, and C which correspond, respectively, to Si  $3p$ –C  $2p$  bonding states (A) and a mixture of Si  $3s$  and C  $2s$  bonding states (B and C) with a slight shift from more Si  $3s$  to more C  $2s$  char-

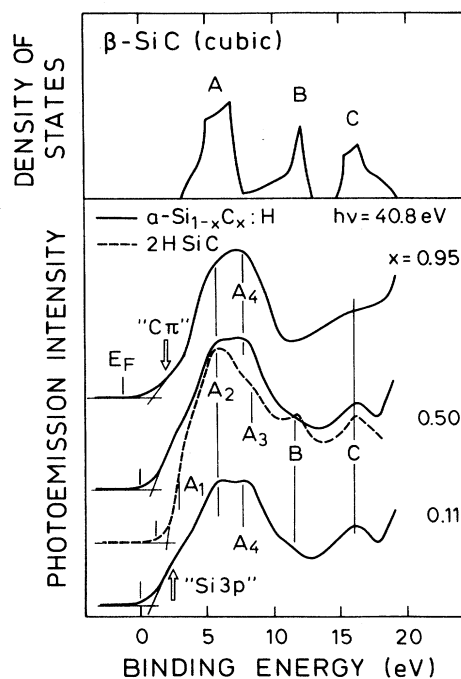


FIG. 1. Valence-band spectra of different  $a\text{-Si}_{1-x}\text{C}_x\text{:H}$  alloys and of crystalline  $2H\text{-SiC}$ . The spectra are aligned at peak C; the position of the valence-band maxima as defined here are indicated by the extrapolations of the leading edges to the base lines; characteristic structures are labeled and their energies are listed in Table I. "C $\pi$ " refers to the C  $2p$   $\pi$ -bonding states. The top panel shows the density of states of cubic SiC as calculated by Robertson (Ref. 30).

acter as one proceeds from B to C.<sup>30–33</sup> The spectrum of  $2H\text{-SiC}$  agrees well with the DOS in the position of these major features as is expected for a covalently bonded semiconductor where the short-range chemical order determines the main features of the electronic structure. The cubic and hexagonal modifications agree in that they contain ordered arrays of Si—C<sub>4</sub> and C—Si<sub>4</sub> tetrahedra without homopolar Si—Si or C—C bonds. The partially ionic character of the Si—C bonds is reflected in the ionic gap between peaks B and C. The fine structure in peak A ( $A_1, A_2, A_3$ ) of the crystalline SiC sample is due to critical points in the DOS for the  $2H$  structure and cannot be

TABLE I. Energies (in eV) of characteristic features in the valence-band spectra ( $h\nu=40.8$  eV) of  $a\text{-Si}_{1-x}\text{C}_x\text{:H}$  alloys and of  $2H\text{-SiC}$ . All energies are referred to peak C in Fig. 1.

Sample	$E_F$	$E(\text{VBM})$	$A_1$	$A_2$	$A_3$	$A_4$	B	C
$a\text{-Si}_{0.89}\text{C}_{0.11}\text{:H}$	15.8	15.0		10.2		8.3	4.4	0
$a\text{-Si}_{0.5}\text{C}_{0.5}\text{:H}$	16.0	15.1	13.2	10.2		8.0	4.4	0
$a\text{-Si}_{0.05}\text{C}_{0.95}\text{:H}$	17.2	14.6		10.2		8.3		0
$2H\text{-SiC}$ (expt.)	14.8	14.0	13.0	10.2	7.6		4.4	0
$2H\text{-SiC}$ (expt.) <sup>a</sup>		14.4		10.6	8.0		4.8	0
$\beta\text{-SiC}$ (theory) <sup>b</sup>		13.0		avg. peak position: 10.3			4.0	0

<sup>a</sup>Reference 35,  $h\nu=151.4$  eV.

<sup>b</sup>Reference 20.

structure and cannot be compared directly with the van Hove singularities in the theoretical DOS of the zinc-blende modification except for points along the symmetry direction  $\Gamma L$  (zinc blende) which map onto the  $\Gamma A\Gamma$  direction in the wurzite structure.<sup>34</sup> The shape of our spectrum agrees quantitatively with that of  $2H$ -SiC ( $\alpha$ -SiC) measured by Parrill and Bermudez<sup>35</sup> if we allow for a rigid shift of  $\sim 0.4$  eV of all features relative to peak C (compare Table I).

For a further discussion of the amorphous valence-band spectra we have to take the differences in photoelectric cross section  $\sigma$  of carbon- and silicon-derived valence states into account. At  $h\nu=40.8$  eV the C  $2p$  cross section is favored over that of the Si  $3p$  states by a factor of about 6 and a somewhat smaller factor of 3.3 applies to  $\sigma(C\ 2s)/\sigma(Si\ 3s)$ .<sup>36</sup> This implies that the photoemission spectra represent essentially the carbon-derived partial density of states. For  $c$ -Si:C this is of little consequence because the Si and C partial DOS carry approximately equal weight over the whole spectrum with only a slight accentuation of the C  $2s$  states in peak C.<sup>30</sup> In going from  $c$ -SiC to the amorphous alloy of the same nominal stoichiometry three elements of disorder must be considered: (i) geometrical disorder, (ii) chemical disorder or the presence of wrong or homonuclear Si—Si and C—C bonds, and (iii) the possibility that carbon forms in addition to the tetrahedrally disposed  $sp^3$  bonds homonuclear  $p\pi$  bonds of various order as in graphite or organic molecules. The influence of Si—H and C—H bonds on the valence-band spectra of our samples is of secondary importance as will be shown later. Geometrical disorder has only a minor effect on the valence-band spectra in that it mainly smears out critical-point structure and introduces tailing at the band edges. The effect of homonuclear bonds on the valence-band spectra is emphasized if we go to the concentration extremes, viz.,  $x=0.11$  and  $x=0.95$ , respectively (see Fig. 1). The  $x=0.11$  spectrum differs from the stoichiometric  $a$ -SiC valence band by a distinct shoulder which we ascribe to the Si  $3p$  bonding states which occur at the top of the valence bands in pure  $a$ -Si (compare also Sec. III C). Part of the shoulder  $A_1$  in the  $a$ -Si<sub>0.5</sub>C<sub>0.5</sub>:H spectrum is likely to be also due to Si-Si  $3p$  bonding states so that the VBM is pushed up in  $a$ -Si<sub>0.5</sub>C<sub>0.5</sub>:H compared to  $2H$ -SiC. At the other extreme ( $x=0.95$ ) a considerable number of C—C bonds are expected which produce feature  $A_4$  that is absent in the  $2H$ -SiC spectrum. Our spectra for  $x>0.6$  look indeed quite similar to those of  $a$ -C:H.<sup>29</sup> A comparison with the valence bands of graphite<sup>37</sup> and diamond<sup>38</sup> further suggests that the pronounced tail at the top of the  $x=0.95$  spectrum is due to  $p\pi$  bonds between carbon atoms in agreement with the theoretical analysis of Robertson.<sup>30-33</sup>

The contribution of hydrogen to the valence-band spectra of our samples has been investigated by annealing the films *in situ* to 650°C, a temperature where, according to the ir spectra hydrogen evolves from Si—H and C—H bonds. After 30 min at this temperature the hydrogen evolution was completed and Fig. 2 shows two representative spectra for high ( $x=0.89$ ) and low ( $x=0.11$ ) carbon content. For the film with high carbon

content virtually no change in the spectral shape has been observed. The complete absence of C-H induced features in the valence-band spectra of  $a$ -Si<sub>1-x</sub>C<sub>x</sub>:H in the high- $x$  regime is corroborated by the results of Katayama *et al.*<sup>29</sup> and Wesner *et al.*<sup>39</sup> on hydrogenated amorphous carbon films. The reason for this absence remains unclear at present.

With increasing Si content Si-H induced features at 6.2 and 11.5 eV binding energy occur which are, of course, best developed in the spectrum of the Si<sub>0.89</sub>C<sub>0.11</sub>:H film in Fig. 2. These features have been identified by von Roedern *et al.*<sup>40</sup> in  $a$ -Si:H with Si  $3p$ -H  $1s$  and Si  $3s$ -H  $1s$  bonding states, respectively. The same peaks have also been observed by Katayama *et al.*<sup>29</sup> in their  $a$ -Si<sub>1-x</sub>C<sub>x</sub>:H ( $x\leq 0.5$ ) alloys prepared at room temperature by the glow-discharge method albeit with an intensity that is at least five times higher than that in our samples. Using the procedure described in Ref. 41 to estimate the hydrogen content of  $a$ -Si:H films from the intensity of the 6.2-eV peak we obtain 10 at. % as an upper limit for the concentration of H atoms bonded to Si in our films with  $x=0.1$  that drops rapidly with increasing  $x$ .

An effect of the removal of hydrogen throughout the concentration range is an increase of the density of states at the top of the valence-band spectra such that the valence-band maximum is pushed towards lower binding energy. The average shift is about 0.5 eV with a slight trend from 0.4 eV for high  $x$  towards 0.6 eV for  $x$  approaching zero as shown in Fig. 3. This shift is not due to a movement of the Fermi level as confirmed by the fixed position of the core levels and the valence-band

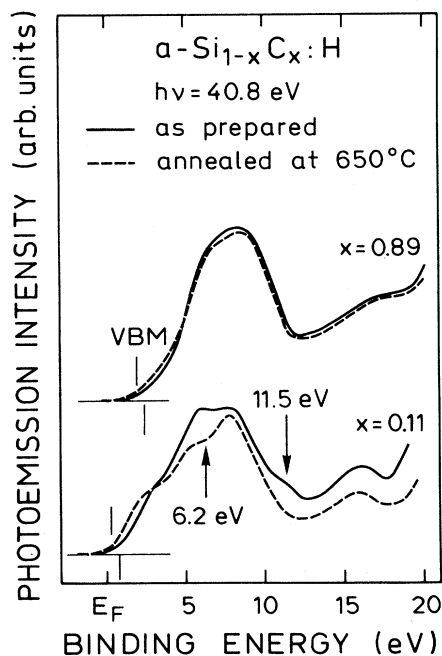


FIG. 2. Valence-band spectra of two alloys before and after annealing at 650°C. The hydrogen-induced features are marked by arrows.

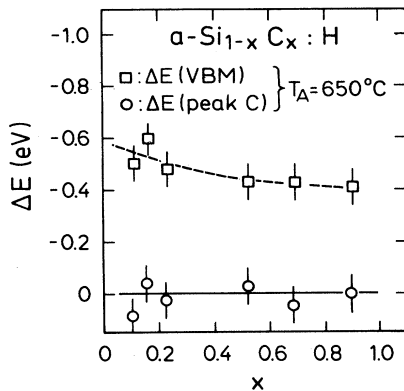


FIG. 3. The change in binding energy of the valence-band maximum and of peak C upon dehydrogenation by annealing at 650°C.

peak C upon annealing (see Fig. 3).

A recession of the valence-band edge upon hydrogenation of *a*-Si of up to 0.7 eV (depending on the hydrogen content) has been reported by Ley *et al.*<sup>42</sup> This is caused by the replacement of the Si—Si bonds by the stronger Si—H bonds and the reduction in the Si—Si coordination number. The same mechanism is certainly responsible for the recession of the VBM in the Si-rich alloys as long as Si—Si bonding states determine the VBM. Whether this mechanism is also responsible for the observed changes in the carbon-rich alloy is a matter of debate. Robertson<sup>30–33</sup> has suggested that hydrogen may affect the size of *sp*<sup>2</sup> bonded (graphitic) carbon clusters, which in turn is responsible for more or less valence-band tailing.

This analysis provides the following information about our *a*-Si<sub>1-x</sub>C<sub>x</sub> films. (i) For *x* < 0.5 a considerable degree of chemical disorder is present as witnessed by the Si 3*p* bonding states which determine the VBM in this concentration range and by the presence of peak *A*<sub>4</sub> which signals C—C bonds. The similarity of the *x* = 0.5 and *x* = 0.11 spectra in Fig. 1 is somewhat misleading, however, because both spectra are governed by the C partial density of states as explained above. Above *x* = 0.5 the number of C—C bonds increases (peak *A*<sub>4</sub> strengthens) and the character of the states at the VBM changes from Si 3*p* to C 2*p* states arising from C—C *pπ* bonds.

#### B. Core-level spectra of *a*-Si<sub>1-x</sub>C<sub>x</sub> (:H)

The change in the network character around *x* = 0.5 is also evident from the core-level binding energies displayed in Fig. 4. For *x* < 0.5 both the Si 2*p* and the C 1*s* binding energies remain virtually unchanged while they increase by ~1 eV (Si 2*p*) and 1.2 eV (C 1*s*) between *x* = 0.5 and *x* = 1 (extrapolated value for Si 2*p*). A parallel trend is observed for feature C of the valence bands. For the top of the valence bands the increase in *E*(VBM) is even stronger, amounting to 2.0 eV between *x* = 0.5 and *x* = 1. As far as the core levels are concerned these observations are in qualitative agreement with similar measurements by Lee<sup>43</sup> and by Katayama *et al.*<sup>44</sup> on glow-discharge samples prepared outside of the spectrometer.

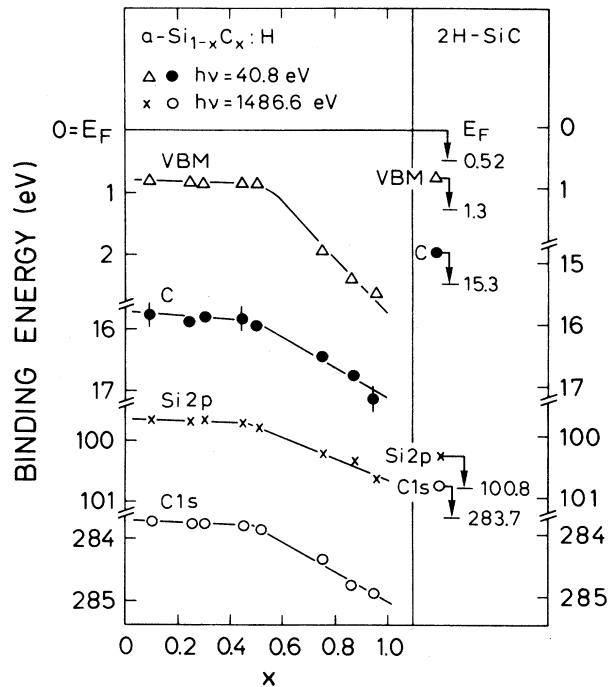


FIG. 4. Binding energies of the valence-band maximum (VBM), peak C, and the Si 2*p* and C 1*s* core levels as a function of carbon content *x*. Also shown on the right-hand side are the same features in 2*H*-SiC both before and after correction for a Fermi-level shift. For details see text.

A meaningful discussion of the energy shifts in Fig. 4 and in particular an answer to the question what to expect for the natural band offsets in the *a*-Si/[*a*-Si<sub>1-x</sub>C<sub>x</sub> (:H)] system is only possible if we are able to separate the Fermi-level shift from the true chemical shifts. Such a separation was achieved in the SiN<sub>x</sub> (Ref. 16) and SiO<sub>x</sub> (Ref. 17) system because N and O occur predominantly in the same chemical environment (i.e., fully Si coordinated) in these alloys and hence their core levels are to first order not chemically shifted. The position of the N 1*s* and O 1*s* core level could thus serve as an internal reference level against which to measure changes in *E*<sub>F</sub>. An independent check of this procedure was performed by deconvoluting the Si 2*p* core-level spectra into their five chemically shifted components Si<sub>*n*</sub> (*n* = 0, 1, . . . , 4) corresponding to the replacement of *n* homopolar Si—Si bonds by the appropriate heteropolar Si—N and Si—O bonds. The movement of the unshifted Si<sub>0</sub> component relative to *E*<sub>F</sub> was found to parallel that of the anion core levels.

Both methods are not applicable in the case at hand. Carbon as well as Si participate in the network in a symmetrical way: Si—Si bonds are replaced by Si—C bonds for increasing *x* and C—C bonds are replaced by C—Si bonds for decreasing *x*. The core levels of both constituents undergo, therefore, chemical shifts and neither can be used to monitor changes in *E*<sub>F</sub>. The difference in the electronegativities of C (Pauling electronegativity 2.5) and Si (1.8), on the other hand, is too small to induce chemical shifts large enough to be analyzed meaningfully with our present resolution.

It is nevertheless possible to deduce the magnitude of the overall Fermi-level shift between  $x=0$  and  $x=1$  by first deducing the chemical shifts of C and Si with the help of the energy scheme of Fig. 5. In Fig. 5 we consider three idealized bonding configurations and the corresponding energy differences  $\Delta_i$  between the C 1s and the Si 2p binding energies. Two cases correspond to the limits  $x \rightarrow 0$  and  $x \rightarrow 1$ , respectively, i.e., to an isolated carbon atom fourfold coordinated in a silicon matrix or a silicon atom in a carbon matrix. The third case, realized in *c*-SiC, is an ordered array of Si atoms fourfold coordinated to C and vice versa. The configurations of the dilute limits are realistic structural models for the Si-C alloy system according to the recent extended x-ray-absorption fine structure (EXAFS) investigations of Kaloyeros *et al.*<sup>45</sup> on samples prepared similarly to ours, i.e., by reactive sputtering. The energy differences are expressed as shown in Fig. 5 in terms of two chemical shifts  $\Delta E_C$  and  $\Delta E_{Si}$ , respectively, and the separation  $E_0$  of the unshifted core levels as a third parameter. Using the same chemical shifts in the dilute limits and the ordered compound implies that we neglect induction effects and differences in final-state relaxation energy for the three bonding configurations. Induction effects, i.e., the influence of the second and further coordination shells on the chemical shifts, have been found to be small in *a*-SiO<sub>x</sub> (Ref. 17) and *a*-SiN<sub>x</sub> (Ref. 16) and are thus expected to be negligible in Si<sub>1-x</sub>C<sub>x</sub> on account of the smaller heteropolarity of the Si—C bond compared to the Si—O and Si—N bonds. In a separate investigation<sup>46</sup> we shall show that the relaxation energy is a local quantity in the sense that it depends almost exclusively on the polarizability of the nearest-neighbor bonds of the photoionized atom. It is therefore included in the chemical shift parameters  $\Delta E_{Si}$  and  $\Delta E_C$ . As energy differences, the quantities  $\Delta_i$  obviously do not depend on the Fermi-level position.

Experimentally, we obtain the following values:

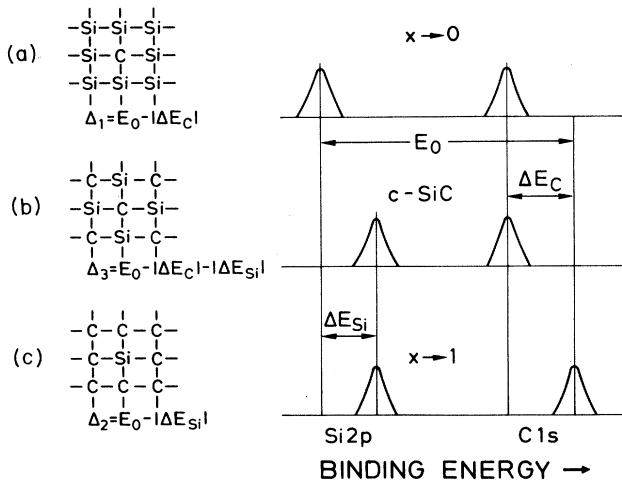


FIG. 5. Three idealized configurations used to calculate the chemical shifts in the Si-C alloy system. For details see text.

$$\begin{aligned}\Delta_1 &= [E(\text{C } 1s) - E(\text{Si } 2p)]_{x \rightarrow 0} \\ &= 283.75 - 99.65 \text{ eV} \\ &= 184.10 \pm 0.05 \text{ eV},\end{aligned}$$

$$\begin{aligned}\Delta_2 &= [E(\text{C } 1s) - E(\text{Si } 2p)]_{x \rightarrow 1} \\ &= 285.04 - 100.65 \text{ eV} \\ &= 184.39 \pm 0.05 \text{ eV},\end{aligned}$$

$$\begin{aligned}\Delta_3 &= [E(\text{C } 1s) - E(\text{Si } 2p)]_{2H\text{-SiC}} \\ &= 283.20 - 100.30 \text{ eV} \\ &= 182.90 \pm 0.05 \text{ eV}.\end{aligned}$$

The errors represent the precision of the energy measurements and the accuracy with which we determine the line positions through least-squares fits. Solving the three expressions in Fig. 5 for  $\Delta E_C$  and  $\Delta E_{Si}$  and using for the  $\Delta_i$  the numerical values just derived we obtain  $\Delta E_C = -(1.43 \pm 0.07)$  eV and  $\Delta E_{Si} = 1.20 \pm 0.07$  eV for the *purely chemical shifts* of the C 1s and Si 2p core levels. These values do not contain any contribution due to a Fermi-level shift. Thus by comparing them with the actually measured increase in the C 1s and Si 2p binding energies between  $x=0$  and  $x=1$  we obtain two independent measures of the overall variation  $\Delta E_F$  in  $E_F$  between the two extreme carbon concentrations:

$$\begin{aligned}\Delta E_F(\text{Si}) &= [E(\text{Si } 2p)]_{x=1} - [E(\text{Si } 2p)]_{x=0} - |\Delta E_{Si}| \\ &= 100.65 - 99.65 - 1.20 \text{ eV} \\ &= -0.20 \pm 0.1 \text{ eV}\end{aligned}$$

from the Si 2p core levels, and

$$\begin{aligned}\Delta E_F(\text{C}) &= [E(\text{C } 1s)]_{x=1} - [E(\text{C } 1s)]_{x=0} - |\Delta E_C| \\ &= 285.04 - 283.75 - 1.43 \text{ eV} \\ &= -0.14 \pm 0.1 \text{ eV}\end{aligned}$$

from the C 1s core-level spectra, respectively.

This means that between  $x=0$  and  $x=1$  the Fermi level shifts away from the valence-band edge by 0.2 eV. The agreement of the two  $\Delta E_F$  values lends strong support to our analysis and the correctness of the underlying model. Without further knowledge about the Fermi-level shift in the intermediate carbon concentration range we assume a linear increase in  $E_F$  between  $x=0$  and  $x=1$ . After this correction the total recession of the VBM with carbon alloying amounts to 2.75 eV. Virtually all of this recession occurs for  $x \geq 0.5$  indicating a profound change in the electronic structure as one goes from a silicon dominated network to one that is rich in carbon. A similarly abrupt transition around  $x=0.5$  has also been observed in ESR and photoluminescence measurements<sup>47</sup> and in the optical data.<sup>48</sup>

The spectral features of 2H-SiC can be made to fit the common core-level-based energy scheme if we allow for a 0.52-eV shift of the Fermi level away from VBM as shown on the right-hand side of Fig. 4. After this correction the Si 2p and C 1s binding energies agree with the

maximally shifted core levels on either end of the concentration range: with  $[E(\text{C } 1s)]_{x=0}$  and  $[E(\text{Si } 2p)]_{x=1}$ .

A word about the energy of the VBM before we turn to the interfaces in the next section. For  $x \leq 0.6$  the VBM was determined by extrapolating the steepest descent of the leading edge of the valence-band spectra to the base line as indicated for  $x = 0.11$  and  $x = 0.5$  in Fig. 1. This is the accepted procedure for crystalline semiconductors and it leads in both instances to values of  $E(\text{VBM})$  that are reproducible to within 0.2 eV. Above  $x = 0.6$  the valence bands start to exhibit an increasing tail at the top of the valence bands which defies this procedure. We have therefore determined  $E(\text{VBM})$  as shown for the worst case ( $x = 0.95$ ) in Fig. 1; i.e., by extrapolating the tail so as to leave about the same amount of integrated photoemission intensity between the extrapolation and the actual spectrum as for  $x < 0.5$ .

With this provision  $E(\text{VBM})$  can be obtained with comparable precision above and below  $x \approx 0.6$ . The ambiguity of defining a valence-band "edge" in an amorphous material remains. For our present purpose this ambiguity does not matter, however, because we use the same  $E(\text{VBM})$  as a measure for the natural band lineup and the actual discontinuity when the interface is formed.

It is clear that our choice of the VBM has not necessarily to do with the energy that determines the optical gap in these systems. An absorption coefficient of  $\sim 10^4 \text{ cm}^{-1}$  which is often taken as characteristic for the optical gap of amorphous systems requires less than a percent of the valence electrons to participate in the optical transitions. This corresponds to a density of states well below that detectable in conventional photoelectron spectroscopy. The great variation in the optical gap of  $a\text{-Si}_{1-x}\text{C}_x$  (:H) above  $x = 0.5$  (Ref. 26) is thus due to the different degree of tailing which we have tried to disregard here to the extent explained above.

### C. Interfaces between $a\text{-Si}$ and $a\text{-Si}_{1-x}\text{C}_x$ (:H)

The valence-band offsets between  $a\text{-Si}$  and different alloys of  $a\text{-Si}_{1-x}\text{C}_x$  (:H) were determined as follows. A layer of pure amorphous silicon was sputtered onto the alloy substrates after the valence band and the Si 2p and C 1s core-level spectra had been measured. The actual deposition commenced by exposing the substrate about 10 min after the discharge had been started in order to stabilize the plasma and remove a possible layer of oxidized silicon from the target. The thickness of the deposited film was controlled through the deposition time after repeated calibration runs with films thick enough so that their thickness could be measured with a Tallysurf.

Valence-band spectra before and after deposition of a 10-Å-thick amorphous Si film on alloys of various compositions are shown in Fig. 6. The spectra of the heterojunctions appear broadly speaking as a superposition of the  $a\text{-Si}$  epilayer and the alloy substrate. The prominent hump at the valence-band top that appears after deposition is readily identified with Si 3p states that govern the  $a\text{-Si}$  valence-band spectrum at this photon energy as seen by the reference spectrum at the bottom of Fig. 6. A change  $\Delta E(\text{VBM})$  in the energy of the VBM of up to 2.5

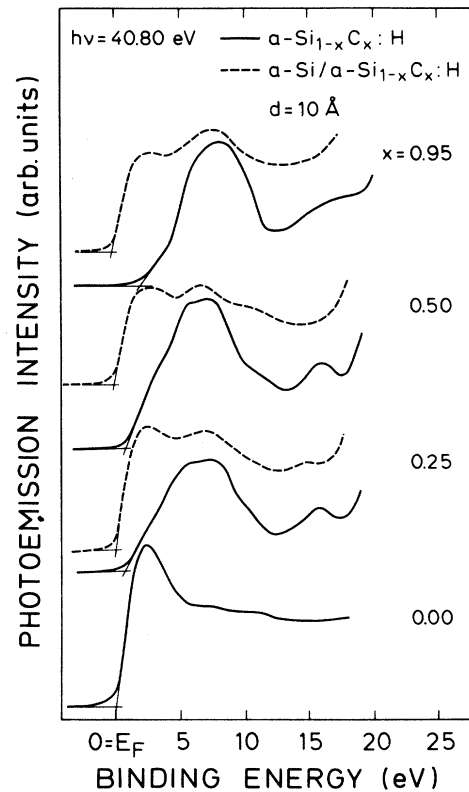


FIG. 6. Valence-band spectra of several  $a\text{-Si}_{1-x}\text{C}_x$  (:H) alloys before and after deposition of a 10-Å-thick  $a\text{-Si}$  epilayer. Also shown at the bottom is the spectrum of pure  $a\text{-Si}$  for comparison.

eV upon interface formation is evident from the spectra. This shift is not directly related to the valence-band offset  $\Delta E_v$  because the energy levels of the substrate might also change relative to  $E_F$  due to an overlayer-induced band bending. We have measured the amount of band bending by monitoring the energy of the C 1s core level as illustrated in Fig. 7. We do indeed observe an overlayer-induced reduction in the C 1s binding energy of 0.55 eV for the sample with  $x = 0.95$  which we attribute to a change in band bending (bands bend upwards, i.e., towards  $E_F$ ) by the same amount. The corrected valence-band offset  $\Delta E_v$  is thus given by

$$\Delta E_v = -\Delta E(\text{VBM}) + \Delta E(\text{C } 1s).$$

The sign convention is such that for the valence-band offsets  $\Delta E_v$  is positive if the  $\Delta E(\text{VBM})$  and the  $\Delta E(\text{C } 1s)$  refer to changes in binding energy (negative in our example).

The values for these parameters and the deduced valence-band offsets for the whole range of carbon concentration are summarized in Fig. 8. A constant valence-band discontinuity of  $0.8 \pm 0.1$  eV is measured for  $x < 0.4$  followed by a linear rise that extrapolates to  $1.95 \pm 0.15$  eV for  $x = 1$ . It is also clear from Fig. 8(a) that measurable band bending sets in at  $x = 0.6$  and appears to level off around 0.6 eV towards  $x = 1$ .

An overlayer thickness of  $d = 10$  Å was chosen to determine  $\Delta E_v$  after the evolution of the valence-band

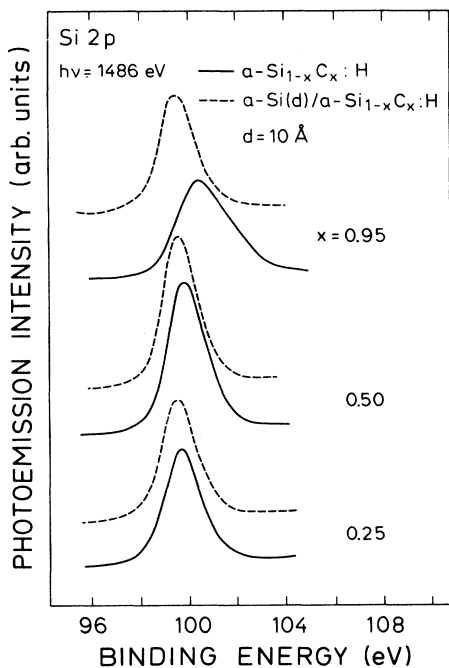


FIG. 7. C 1s core-level spectra before and after interface formation.

discontinuity had been studied for a number of systems. The valence-band spectra for the  $a\text{-Si}/a\text{-Si}_{0.1}\text{C}_{0.9}\text{:H}$  system are shown in Fig. 9 while the relevant energies are plotted as a function of  $d$  in Fig. 10. The VBM is seen to move continuously up to about  $d \approx 20$  Å. This shift is a combination of a Fermi-level shift due to overlayer-induced band bending as monitored by the C 1s binding energy [ $\Delta E(\text{C } 1s)$ ] and the actual valence-band discontinuity  $\Delta E_v$  (compare Fig. 10).  $\Delta E_v$  as the difference between  $\Delta E(\text{VBM})$  and  $\Delta E(\text{C } 1s)$  is seen to remain constant above  $d = 10$  Å, which corresponds to about 4–5 Si monolayers. Below that value the Si valence-band structure is obviously not yet fully developed as can be seen by comparing the top parts of the  $d = 8$  with the  $d = 10$  Å

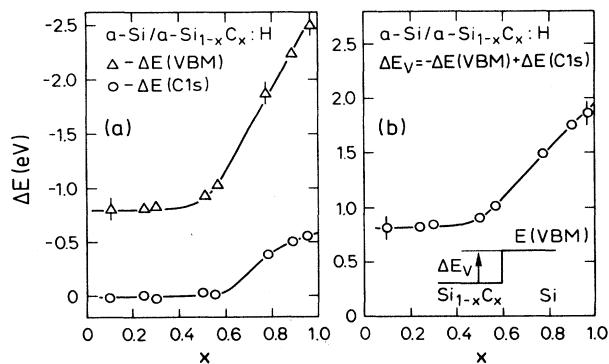


FIG. 8. (a) Changes in the binding energies of the valence-band maximum [ $\Delta E(\text{VBM})$ ] and of the C 1s core level [ $\Delta E(\text{C } 1s)$ ] upon interface formation as a function of carbon content  $x$ . (b) The valence-band offset  $\Delta E_v$  derived from the data of (a).

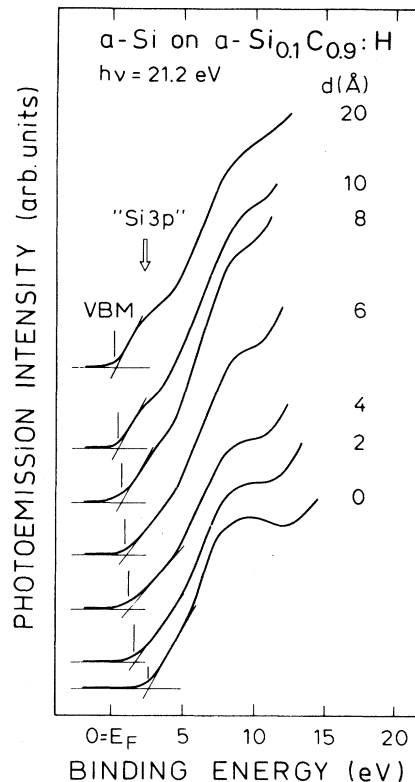


FIG. 9. Valence-band spectra that show the evolution of the  $a\text{-Si}/a\text{-Si}_{0.1}\text{C}_{0.9}\text{:H}$  interface as a function of overlayer thickness  $d$ .

spectra in Fig. 9. Katnani<sup>49</sup> arrived at a similar minimum coverage for the crystalline Ge on GaAs interface, whereas Yang *et al.*<sup>50</sup> observed that the valence-band discontinuity in the  $a\text{-Si:H}/a\text{-SiO}_x\text{:H}$  system was already fully developed at a coverage of only 2 Å. Island formation of the overlayer as a possible cause for the slow saturation of  $\Delta E_v$  has been excluded in our case. The in-

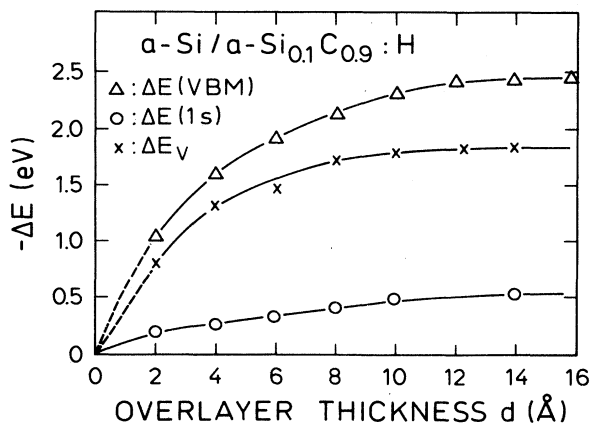


FIG. 10. Variation in the position of the valence-band maximum [ $\Delta E(\text{VBM})$ ], the C 1s core-level binding energy [ $\Delta E(\text{C } 1s)$ ], and the valence-band discontinuity  $\Delta E_v$  as a function of overlayer thickness for the sample of Fig. 9.

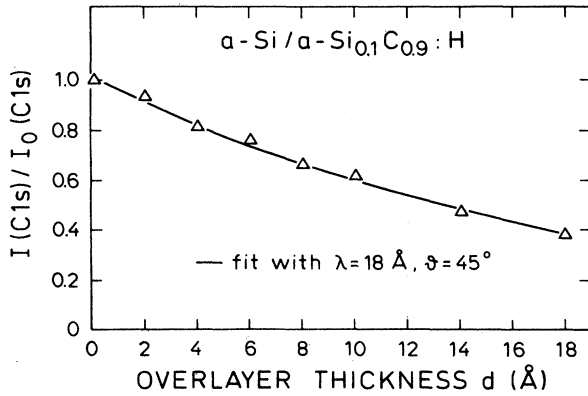


FIG. 11. Attenuation of the intensity of the C 1s signal as a function of overlayer thickness. The solid line is a fit to the data appropriate for a homogeneous overlayer and an electron mean free path of 18 Å.

tensity of the C 1s signal of the underlying Si-C alloy follows the exponential attenuation

$$I(C\ 1s) = I_0(C\ 1s)e^{-d/\lambda \sin\theta}$$

as a function of overlayer thickness expected for a homogeneous growth of the *a*-Si overlayer as shown in Fig. 11. The angle  $\theta$  is the average escape angle of photoelectrons in our spectrometer. A value of 18 Å for the electron mean free path obtained from a least-squares fit to the above expression to the data points is expected for photoelectrons with a kinetic energy of  $\sim 1200$  eV.<sup>51</sup> Because the differences in the evaluation of the *a*-Si:H/*a*-SiO<sub>x</sub>:H and the *a*-Si/*a*-Si<sub>1-x</sub>C<sub>x</sub>:H interfaces are not the subject matter of this investigation we close this section with the general remark that in all our samples the valence-band offset was stable beyond a nominal overlayer thickness of 10 Å.

#### IV. DISCUSSION

The stated purpose of this investigation is to compare actually measured valence-band offsets in the *a*-Si/[*a*-Si<sub>1-x</sub>C<sub>x</sub>(:H)] system with what we termed the natural offset  $\Delta E_v^0$ . The natural offset is obtained when the valence-band maxima of *a*-Si and *a*-Si<sub>1-x</sub>C<sub>x</sub>:H are aligned as shown in Fig. 12(b) such that the chemically unshifted components of the Si 2*p* spectrum (Si<sub>0</sub> 2*p*) coincide in energy. For *a*-Si prepared by sputtering at room temperature  $E(\text{VBM}) - E(\text{Si}_0\ 2p) = -(99.6 \pm 0.1)$  eV. In Fig. 13(a) we plot

$$\begin{aligned} \Delta E_v^0 &= [E(\text{VBM}) - E(\text{Si}_0\ 2p)]_{\text{alloy}} \\ &\quad - [E(\text{VBM}) - E(\text{Si}_0\ 2p)]_{a\text{-Si}} \\ &= [E(\text{VBM}) - E(\text{Si}_0\ 2p)]_{\text{alloy}} + 99.6\ \text{eV} \end{aligned}$$

as a function of alloy composition (solid dots). The solid dots are obtained from Fig. 4 taking  $[E(\text{Si}\ 2p)]_{x \rightarrow 0} = E(\text{Si}_0\ 2p)$  and after correcting  $E(\text{VBM})$  for the Fermi-level shift as described in Sec. III B. Also included in

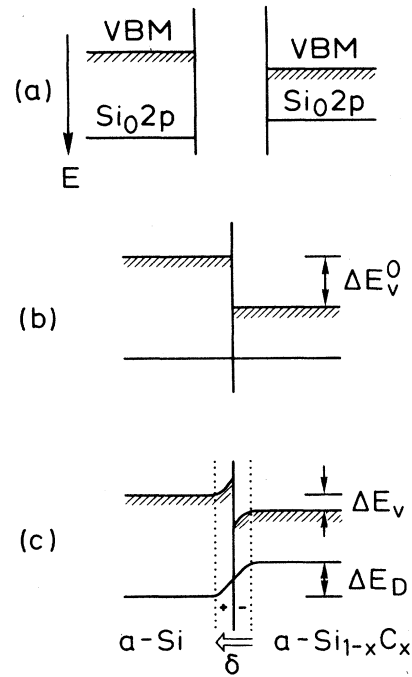


FIG. 12. Schematic energy diagram of the *a*-Si/[*a*-Si<sub>1-x</sub>C<sub>x</sub>(:H)] interface. (a) before joining the two materials; (b) the natural band offset  $\Delta E_v^0$  when the unshifted Si 2*p* core-level components (Si<sub>0</sub> 2*p*) line up; (c) the presence of an interface dipole layer of areal density  $\delta$  reduces  $\Delta E_v^0$  by  $\Delta E_D$  to  $\Delta E_v$ .

Fig. 13(a) are the measured valence-band discontinuities  $\Delta E_v$  in the form  $\Delta E_v^0 - \Delta E_v$  (open circles). The error bars on these points represent the combined error of  $\Delta E_v$  and  $E(\text{VBM}) - E(\text{Si}_0\ 2p)$  excluding the systematic uncertainty in determining  $E(\text{VBM})$  for  $x \geq 0.6$  for the reasons stated earlier (compare Sec. III A). From this figure the following conclusions can be drawn.

(i) The natural band offset correctly predicts the valence-band discontinuity within the experimental limits of accuracy up to  $x \approx 0.5$ . For higher carbon concentrations the deviations between  $\Delta E_v^0$  and  $\Delta E_v$  increase up to 0.7 eV, which amounts to about 30% of the natural offset at  $x = 1$ .

(ii) The nonvanishing offset at  $x = 0$  is due to the hydrogen-induced recession of the VBM in the alloys. This becomes evident in Fig. 13(b) where we compare the natural offset between *a*-Si and dehydrogenated *a*-Si<sub>1-x</sub>C<sub>x</sub>. The values for  $E(\text{VBM}) - E(\text{Si}_0\ 2p)$  are taken again from Fig. 4 using the interpolated extension of the VBM upon dehydrogenation from Fig. 2. The actual band offset was measured for a few interfaces as indicated in Fig. 13(b) by the open circles. Again we find reasonable agreement between  $\Delta E_v^0$  and  $\Delta E_v$  for small  $x$  and a reduced offset for  $x \geq 0.5$ . The finite offset between the two nominally identical samples of unhydrogenated *a*-Si in Fig. 13(b) is due to the differences in preparation. Annealing the hydrogenated *a*-Si<sub>1-x</sub>C<sub>x</sub>:H ( $x \rightarrow 0$ ) sample at  $T_a = 650^\circ\text{C}$  reduces the disorder-induced valence-band tail in the sample prepared at RT by  $\sim 0.2$  eV. By implication we expect a vanishing valence-band discontinuity

between  $a\text{-Si:H}$  and  $a\text{-Si}_{1-x}\text{C}_x\text{:H}$  for  $x \leq 0.5$  if both are prepared at the same substrate temperature and with the same hydrogen content in agreement with published cases.<sup>25,52</sup>

At this stage we might ask whether a dipole layer at the interface might be responsible for the difference between  $\Delta E_v^0$  and  $\Delta E_v$ . According to simple physical intuition which is confirmed by detailed calculations on crystalline systems<sup>4</sup> we expect an interface dipole such that negative charge is displaced towards the material with the higher average electronegativity. This would be  $\text{Si}_{1-x}\text{C}_x\text{:H}$  in our case and the ensuing situation is depicted schematically in Fig. 12(c). With this orientation the dipole layer would reduce the valence-band offset by an amount of  $\Delta E_D$  as is observed experimentally. The reduction depends on the magnitude of the dipole area

density  $\delta$  according to

$$|\Delta E_D| = \frac{1}{\epsilon\epsilon_0} |\delta|.$$

With a dielectric constant of  $\epsilon = 8.7$  (average between Si,  $\epsilon = 11.7$ , and C (diamond),  $\epsilon = 5.7$ ) this yields in the limit  $x \rightarrow 1$  ( $\Delta E_D = 0.7$  eV)  $\delta = 3.4 \times 10^{14}$  ( $e \text{ \AA}/\text{cm}^2$ ). The polarizable entities are the atoms with an approximate area density of  $\sim 8 \times 10^{14} \text{ cm}^{-2}$  per monolayer so that the individual dipoles amount to  $\sim 4 \times 10^{-1} e \text{ \AA}$ . Assuming further as suggested by the calculations alluded to above that the dipoles extend essentially over one or two interatomic distances we arrive at a transfer of  $1 \times 10^{-2}$  elementary charges over a typical dipole length of 4  $\text{\AA}$ . This value is comparable to the charge calculated by Christensen for a number of crystalline interfaces.<sup>4</sup>

It thus appears that our analysis provides direct evidence for a dipole layer that affects the band lineup of the  $a\text{-Si}/a\text{-Si}_{1-x}\text{C}_x\text{:H}$  interface. This interpretation is further supported by the diminishing magnitude of  $\Delta E_v - \Delta E_v^0$  as  $x$  tends towards zero. As the average ionicity of the two materials approach each other the charge transfer and with it the dipole density decreases and the valence-band discontinuity tends towards its natural value. This is a nontrivial result in the case of hydrogenated  $a\text{-Si}_{1-x}\text{C}_x$  because the valence-band offset remains finite and rather large (0.8 eV) as  $x$  goes to zero. This offset is due to the reduced valence-band width of hydrogenated amorphous silicon and its diluted alloys which has been alluded to earlier. We also find that the dipole contribution to the valence-band discontinuity remains the same after dehydrogenation of  $a\text{-Si}_{1-x}\text{C}_x\text{:H}$  ( $x \geq 0.6$ ) [compare Figs. 13(a) and 13(b)]. Again this is to be understood in the framework of our model if hydrogen affects the valence-band maximum as discussed in Sec. III A without appreciably changing the average ionicity of the alloy on account of its low concentration. One might ask, however, why the dipole contribution to  $\Delta E_v$  appears to set in only above  $x \approx 0.5$ . We think that this is due to our way to correct for the Fermi-level shift. Recall that we distributed the overall Fermi-level shift of 0.2 eV between  $x = 0$  and  $x = 1$  equally over the carbon concentration range. Had we, for example, assumed that  $E_F$  starts to shift no earlier than  $x = 0.6$  then  $\Delta E_D = \Delta E_v - \Delta E_v^0$  in Fig. 13 would begin to deviate from zero earlier without affecting the maximum value of  $\Delta E_D$  ( $x \rightarrow 1$ ). An initial downward shift ( $E_F$  moves towards VBM) would enhance this effect.

Let us finally comment on the contributions of the dipole layer and band bending on the C 1s line. The transfer of negative charge towards the  $\text{Si}_{1-x}\text{C}_x\text{:H}$  on account of the dipole layer [compare Fig. 14(c)] tends to reduce the C 1s binding energy; it acts thus in the same direction as the band bending [see Fig. 8(a)]. However, the dipole layer is confined to the first one or two atomic planes at the interface whereas the band bending extends at least over several hundred angstroms. Therefore, only a small fraction of the carbon atoms contributing to the photoelectron spectroscopy (PES) spectrum will exhibit the extra dipole-induced shift. This fraction is

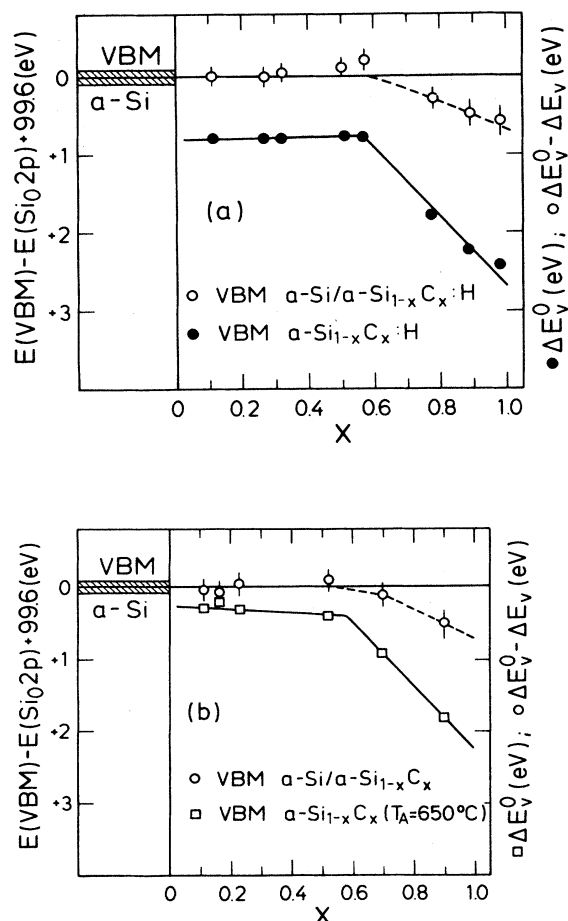


FIG. 13. The valence-band maximum plotted as a function of carbon content  $x$  relative to the unshifted Si  $2p$  component for (a) hydrogenated and (b) dehydrogenated Si-C alloys. The energy scale is chosen in such a way that zero corresponds to  $E(\text{VBM})$  for  $a\text{-Si}$ . In this way the values for  $E(\text{VBM})$  give directly the natural offset  $\Delta E_v^0$ . The open circles are obtained by subtracting the measured valence-band offset  $\Delta E_v$  from  $\Delta E_v^0$ . The hatched region in (a) and (b) indicates the reproducibility of  $E(\text{VBM}) - E(\text{Si}_0 2p)$  in  $a\text{-Si}$ .

$$f = \frac{I_D}{I_0} = 1 - e^{-l/(2\lambda \sin\theta)},$$

where  $I_D$  and  $I_0$  refer to the dipole affected and the total line intensity, respectively. Taking for the effective electron mean free path  $\lambda \sin\theta$  the same value deduced earlier for the Si  $2p$  electrons in  $a$ -Si ( $\lambda \sin 45^\circ = 13 \text{ \AA}$ ) and for half the dipole length  $l/2 = 2.0 \text{ \AA}$  we obtain  $f = 0.14$ . That means that only 14% of the total line intensity is affected by the interface dipole. The effect is therefore small and tends, if anything, to increase the correction ascribed in our analysis to band bending. A reduced band bending would in turn increase  $\Delta E_v$  (compare Fig. 8) and bring the actual valence-band offset closer to that expected without interface dipoles. Our estimate of the contribution of an interface dipole to the valence-band offset is in this sense an upper limit.

### V. SUMMARY AND CONCLUSION

In summary, we have measured the valence-band discontinuity  $\Delta E_v$  at the  $a$ -Si/[ $a$ -Si $_{1-x}$ C $_x$  (:H)] interface over the full range of carbon concentration from  $x = 0$  to  $x \approx 1$ .  $\Delta E_v$  increases with  $x$  from 0.8 to 2.0 eV for hydrogenated Si $_{1-x}$ C $_x$ :H alloys and from 0.25 to 1.5 eV for dehydrogenated Si $_{1-x}$ C $_x$  alloys annealed at 650 °C. We compare these values with the so-called natural valence-band offsets  $\Delta E_v^0$  which we obtain by referring the valence-band maxima of the individual components forming the interface to the chemically unshifted component of the Si  $2p$  core level as a common reference level.

For  $x \lesssim 0.5$ ,  $\Delta E_v^0$  and  $\Delta E_v$  agree to within the experimental uncertainty of  $\pm 0.15$  eV. Above  $x \approx 0.5$ , the actual offsets start to deviate from  $\Delta E_v^0$  in proportion to the carbon content in such a way that the measured offset is smaller than  $\Delta E_v^0$ . The maximum difference amounts to about 30% of  $\Delta E_v^0$ , for  $x \rightarrow 1$ . The sign of the reduction and its increase with carbon content is compatible with an interpretation in terms of an interface dipole layer brought about by a polarization of bond charges in the direction of the Si $_{1-x}$ C $_x$  layer which is on the average more electronegative than silicon. The magnitude of the areal interface dipole density necessary to explain the ob-

served differences between  $\Delta E_v$  and  $\Delta E_v^0$  ( $3.4 \times 10^{14} \text{ e \AA/cm}^2$ ) is comparable to that calculated by Christensen for typical crystalline interface dipoles.<sup>4</sup>

This result requires a few qualifying remarks. As has been pointed out by van der Walle *et al.*<sup>2,3</sup> and others the magnitude of the interface dipole depends on the reference surfaces chosen for the free surfaces before forming the interface. The unshifted Si $_0$   $2p$  core-level component as a reference level might have been a particularly fortunate choice in our case. The binding energy of Si $_0$   $2p$  probes the potential inside a sphere which contains the basic Si-Si $_4$  tetrahedron responsible for the Si $_0$   $2p$  component. Across the surface of this sphere we can envisage dipoles that are set up by the ionicity of the bonds connecting the Si-Si $_4$  tetrahedron to the remainder of the Si $_{1-x}$ C $_x$  network. These dipoles have the same origin and direction as those formed at the interface and we would argue that our choice of reference level accounts, therefore, already for some of the charge transfer at the interface. This would explain the remarkable agreement between  $\Delta E_v$  and  $\Delta E_v^0$  over much of the concentration range. Clearly, a study of interfaces of systems with a larger electronegativity difference such as Si/SO $_x$  would be desirable. Our study has also demonstrated that amorphous systems are ideally suited for this kind of work because they give large band discontinuities and allow a systematic variation of band-edge positions and average ionicities. To take full advantage of these properties it is mandatory, however, to perform the determination of band offsets and band-edge positions on the same sample. Otherwise, the uncertainty in defining a band edge in an amorphous system offsets much of the gain in accuracy due to the large discontinuities.

### ACKNOWLEDGMENTS

We thank N. Christensen and J. Robertson for many very helpful discussions, and R. Helbig, University of Erlangen, for the gift of a SiC crystal. The technical support by W. Stiepany and J. Feichtinger is appreciated. One of us (R.-C.F.) thanks the Max Planck Society for financial support and Professor M. Cardona for his hospitality. This work was supported by Der Bundesminister für Forschung und Technologie under No. 0328 962 A.

\*Permanent address: University of Science and Technology of China, Hefei 230 029, Anhui, P.R. China.

†Present address: Institut für Technische Physik, Universität Erlangen-Nürnberg, D-8520 Erlangen, F.R.G.

<sup>1</sup>For a recent compilation of experimental band discontinuities, see G. Margaritondo and P. Perfetti, in *Heterojunction Band Discontinuities*, edited by F. Capasso and G. Margaritondo (North-Holland, Amsterdam, 1987), p. 72ff.

<sup>2</sup>C. G. van der Walle and R. M. Martin, *Phys. Rev. B* **34**, 5621 (1986).

<sup>3</sup>C. G. van der Walle and R. M. Martin, *Phys. Rev. B* **35**, 8145 (1987).

<sup>4</sup>N. E. Christensen, *Phys. Rev. B* **37**, 4528 (1988).

<sup>5</sup>N. E. Christensen, *Phys. Rev. B* **38**, 12 687 (1988).

<sup>6</sup>R. W. Grant, E. A. Kraut, J. R. Waldrop, and S. P.

Kowalczyk, in Ref. 1, p. 167.

<sup>7</sup>F. Flores and C. Tejedor, *J. Phys. C* **12**, 731 (1979).

<sup>8</sup>J. Tersoff, *Phys. Rev. B* **30**, 4874 (1984).

<sup>9</sup>M. Cardona and N. E. Christensen, *Phys. Rev. B* **35**, 6182 (1987).

<sup>10</sup>W. A. Harrison, *J. Vac. Sci. Technol.* **14**, 1016 (1977).

<sup>11</sup>W. A. Harrison and J. Tersoff, *J. Vac. Sci. Technol. B* **4**, 1068 (1986).

<sup>12</sup>R. L. Anderson, *Solid-State Electron.* **5**, 341 (1962).

<sup>13</sup>J. M. Langer and H. Heinrich, *Phys. Rev. Lett.* **55**, 1414 (1985); *Physica* **134B**, 444 (1985).

<sup>14</sup>M. J. Caldas, A. Fazzio, and A. Zunger, *Appl. Phys. Lett.* **45**, 671 (1984).

<sup>15</sup>C. K. Shih and W. E. Spicer, *Phys. Rev. Lett.* **58**, 2594 (1987).

<sup>16</sup>R. Kärcher, L. Ley, and R. L. Johnson, *Phys. Rev. B* **30**, 1896

- (1984).
- <sup>17</sup>F. G. Bell and L. Ley, *Phys. Rev. B* **37**, 8383 (1988); in this paper a natural valence-band offset of 4.5 eV was predicted for the *a*-Si/[*a*-SiO<sub>2</sub> (:H)] interface; this value has to be reduced by about 0.7 eV when the interface between *a*-Si:H and *a*-SiO<sub>2</sub> (:H) is considered (compare Ref. 16).
- <sup>18</sup>B. Abeles, I. Wagner, W. Eberhardt, J. Stöhr, H. Stasiewski, and F. Sette, in *Optical Effects in Amorphous Semiconductors*, Proceedings of the International Topical Conference on Optical Effects in Amorphous Semiconductors, AIP Conf. Proc. No. 120, edited by P. G. Taylor and S. G. Bishop (AIP, New York, 1984), p. 394.
- <sup>19</sup>C. Colluza, G. Fortunato, C. Quaresima, M. Capozzi, and P. Perfetti, *J. Non-Cryst. Solids* **77&78**, 999 (1985).
- <sup>20</sup>L. Yang, B. Abeles, W. Eberhardt, H. Stasiewski, and D. Sondericker, *Phys. Rev. B* **35**, 9395 (1987).
- <sup>21</sup>J. Menéndez, *Phys. Rev. B* **38**, 6305 (1988).
- <sup>22</sup>P. Zurcher and R. S. Bauer, *J. Vac. Sci. Technol.* **21**, 498 (1982).
- <sup>23</sup>D. W. Niles and G. Margaritondo, *Phys. Rev. B* **34**, 2923 (1986).
- <sup>24</sup>J. Robertson (private communication); these values supersede the ones given in J. Robertson, *J. Non-Cryst. Solids* **97&98**, 863 (1987).
- <sup>25</sup>F. Evangelisti, *J. Non-Cryst. Solids* **77&78**, 969 (1985).
- <sup>26</sup>For a recent review see, e.g., J. Bullo and M. P. Schmidt, *Phys. Status Solidi B* **143**, 345 (1987).
- <sup>27</sup>H. Wieder, M. Cardona, and C. R. Guarnieri, *Phys. Status Solidi B* **92**, 99 (1979).
- <sup>28</sup>F. Fujimoto, A. Ootuka, K. Komaki, Y. Iwata, I. Yamane, H. Yamashita, Y. Hashimoto, Y. Tawada, K. Nishimura, H. Okamoto, and Y. Hamakawa, *Jpn. J. Appl. Phys. Pt. 1* **23**, 810 (1984).
- <sup>29</sup>Y. Katayama, T. Shimada, K. Kobayashi, C. Jiang, H. Daimon, and Y. Murata, *Physica* **117&118B**, 947 (1983).
- <sup>30</sup>J. Robertson (private communication).
- <sup>31</sup>J. Robertson, *Adv. Phys.* **35**, 317 (1986).
- <sup>32</sup>J. Robertson and E. O'Reilly, *Phys. Rev. B* **35**, 2946 (1987).
- <sup>33</sup>J. Robertson, *Philos. Mag. Lett.* **57**, 143 (1988).
- <sup>34</sup>J. L. Birman, *Phys. Rev.* **115**, 1493 (1959).
- <sup>35</sup>T. M. Parrill and V. M. Bermudez, *Solid State Commun.* **63**, 231 (1987).
- <sup>36</sup>S. M. Goldberg, C. S. Fadley, and S. Kono, *J. Electron Spectrosc. Relat. Phenom.* **21**, 285 (1981).
- <sup>37</sup>A. Bianconi, S. B. M. Hagström, and R. Z. Bachrach, *Phys. Rev. B* **16**, 5543 (1977).
- <sup>38</sup>B. B. Pate, W. E. Spicer, T. Ohta, and I. Lindau, *J. Vac. Sci. Technol.* **17**, 1987 (1980).
- <sup>39</sup>D. Wesner, S. Krümmacher, R. Carr, T. K. Sham, M. Strongin, W. Eberhardt, S. L. Weng, G. Williams, M. Howells, F. Kampas, S. Heald, and F. W. Smith, *Phys. Rev. B* **28**, 2152 (1983).
- <sup>40</sup>B. von Roedern, L. Ley, and M. Cardona, *Phys. Rev. Lett.* **39**, 1576 (1977).
- <sup>41</sup>L. Ley, in *Hydrogenated Amorphous Silicon*, Vol. 56 of *Topics in Applied Physics*, edited by J. D. Joannopoulos and G. Lucovsky (Springer, Heidelberg, 1984), p. 92.
- <sup>42</sup>L. Ley, J. Reichardt, and R. L. Johnson, in *Proceedings of the 17th International Conference on the Physics of Semiconductors, San Francisco, 1984*, edited by J. D. Chadi, W. A. Harrison (Springer, New York, 1985), p. 811.
- <sup>43</sup>W.-Y. Lee, *J. Appl. Phys.* **51**, 3365 (1980).
- <sup>44</sup>Y. Katayama, K. Usami, and T. Shimada, *Philos. Mag. B* **43**, 283 (1981).
- <sup>45</sup>A. E. Kaloyeros, R. B. Rizk, and J. B. Woodhouse, *Phys. Rev. B* **38**, 13 099 (1988).
- <sup>46</sup>L. Tang and L. Ley (unpublished).
- <sup>47</sup>S. Liedtke, K. Jahn, F. Finger, and W. Fuhs, *J. Non-Cryst. Solids* **97&98**, 1083 (1987).
- <sup>48</sup>J. Sotiropoulos and G. Weiser, *J. Non-Cryst. Solids* **97&98**, 1087 (1987).
- <sup>49</sup>A. D. Katnani, in Ref. 1, p. 115.
- <sup>50</sup>L. Yang, B. Abeles, W. Eberhardt, and H. Stasiewski, *Phys. Rev. B* **35**, 9395 (1987).
- <sup>51</sup>C. R. Brundle, *Surf. Sci.* **48**, 99 (1975).
- <sup>52</sup>Y. Okayasu, K. Fukui, and M. Matsumura, *Appl. Phys. Lett.* **50**, 248 (1987).